Wavefront sensing of atmospheric phase distortions at the Palomar 200 " telescope and implications for adaptive optics

Bloemhof, Eric, Westphal, James, Ewald, S.

Eric E. Bloemhof, James A. Westphal, S. P. Ewald, "Wavefront sensing of atmospheric phase distortions at the Palomar 200" telescope and implications for adaptive optics," Proc. SPIE 3125, Propagation and Imaging through the Atmosphere, (23 September 1997); doi: 10.1117/12.283893

SPIE.

Event: Optical Science, Engineering and Instrumentation '97, 1997, San Diego, CA, United States

Wavefront Sensing of Atmospheric Phase Distortions at the Palomar 200" Telescope and Implications for Adaptive Optics

E. E. Bloemhof, J. A. Westphal, and S. P. Ewald

California Institute of Technology
Pasadena, CA 91125

ABSTRACT

Major efforts in astronomical instrumentation are now being made to apply the techniques of adaptive optics to the correction of phase distortions induced by the turbulent atmosphere and by quasi-static aberrations in telescopes themselves. Despite decades of study, the problem of atmospheric turbulence is still only partially understood. We have obtained video-rate (30 Hz) imaging of stellar clusters and of single-star phase distortions over the pupil of the 200" Hale telescope on Palomar Mountain. These data show complex temporal and spatial behavior, with multiple components arising at a number of scale heights in the atmosphere; we hope to quantify this behavior to ensure the feasibility of adaptive optics at the Observatory. We have implemented different wavefront sensing techniques to measure aperture phase in wavefronts from single stars, including the classical Foucault test, which measures the local gradient of phase, and the recently-devised curvature sensing technique, which measures the second derivative of pupil phase and has formed the real-time wavefront sensor for some very productive astronomical adaptive optics. Our data, though not fast enough to capture all details of atmospheric phase fluctuations, provide important information regarding the capabilities that must be met by the adaptive optics system now being built for the 200" telescope by a team at the Jet Propulsion Lab. We describe our data acquisition techniques, initial results from efforts to characterize the properties of the turbulent atmosphere at Palomar Mountain, and future plans to extract additional quantitative parameters of use for adaptive optics performance predictions.

KEYWORDS: astronomy, atmosphere, telescope, turbulence

1. INTRODUCTION: THE TURBULENT ATMOSPHERE AND ITS EFFECT ON ASTRONOMICAL OBSERVATIONS

Scientific progress in astronomy has generally come as a direct result of technological advances that have had as their goal the improvement of two main instrumental parameters: spatial resolution and sensitivity. Moreover, the operational design of grating spectrometers, which are the workhorse instruments for moderate- and high-resolution work at optical and near-infrared wavelengths, is such that improved spatial resolution translates directly into improved spectral resolution. The performance gains in these areas over the last decade or two, as a result of technological advances such as improved detectors, space-based observing platforms, and new-generation large-aperture telescopes, have produced a "golden age" of scientific discovery at almost every wavelength.

At optical and near-infrared wavelengths, the traditional limiting factor for both spatial resolution and sensitivity is the earth's atmosphere. For ground-based telescopes, the resolution corresponding to the diffraction limit of the telescope optics is never achieved, being typically one or two orders of magnitude smaller than the arc-second "seeing" blur induced by atmospheric turbulence. Modern CCD detectors operate near their theoretical sensitivity limits, and can be fabricated in large formats to image large fields simultaneously, so one may expect only modest sensitivity gains in future from detector improvements. Larger telescope apertures can still gather more light and thus enhance sensitivity, but at great expense; an equal gain in sensitivity could be made by concentrating the collected light onto a smaller spot in the focal plane, but again the turbulent atmosphere limits this to spots far larger than the diffraction limit.

SPIE Vol. 3125 • 0277-786X/97/$10.00

Basing telescopes in space is only a partial solution at present because cost considerations permit only modest apertures to be placed on orbital platforms. What is needed is a way to circumvent the effects of the turbulent atmosphere on wavefronts reaching the apertures of the new generation of large ground-based (8-10 meter) telescopes that are now in use or under construction. Considerable effort is now being invested in the construction of adaptive optics modules that are capable of sensing phase aberrations over the telescope pupil and correcting them on millisecond timescales; although such systems are complex and relatively expensive, they have delivered very promising initial results in actual field use on telescopes.

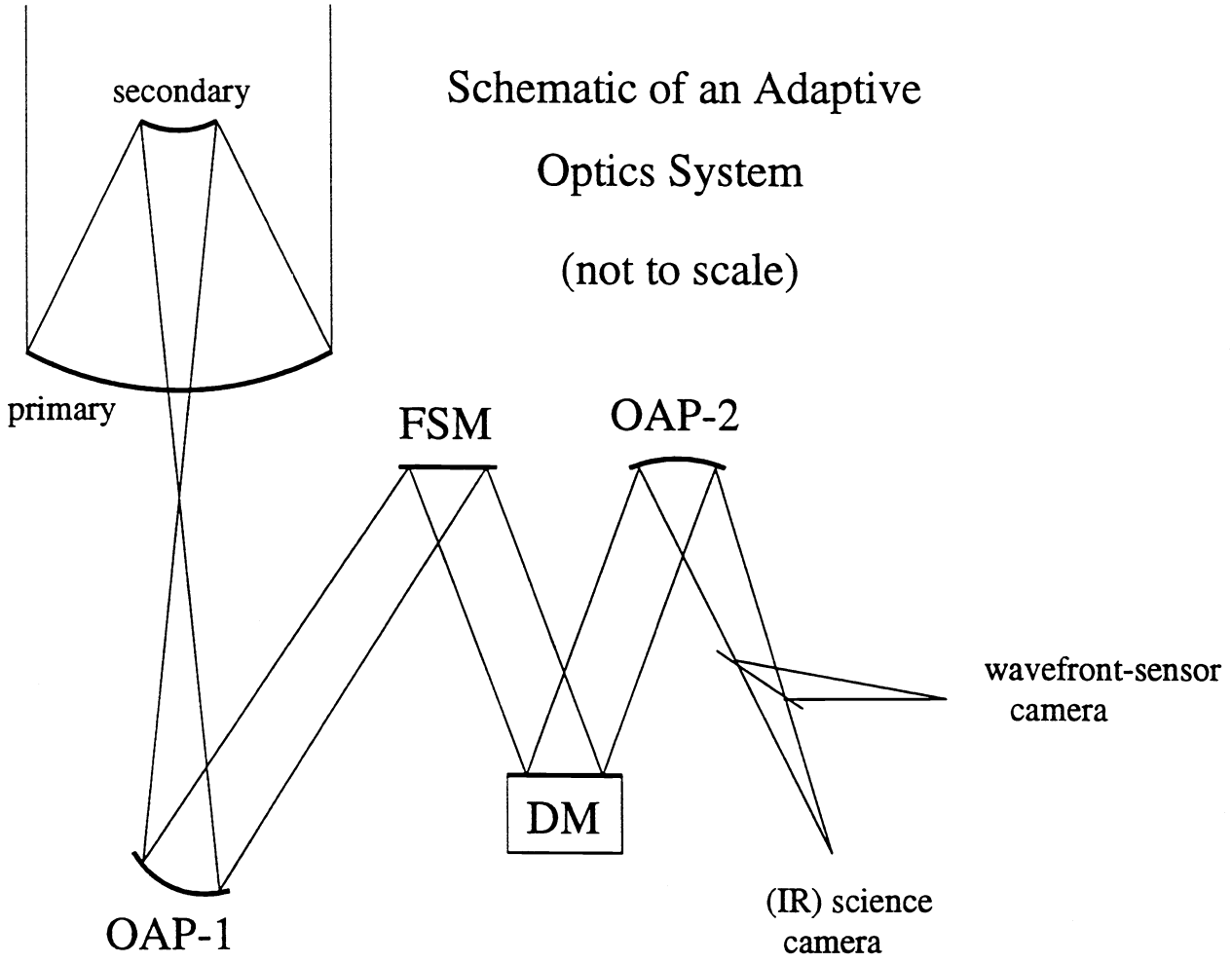

FIG. 1 – Schematic of an astronomical adaptive optics system. Light from the source of interest and from a nearby point reference source is focused into the adaptive optics system by the primary and secondary mirrors of the telescope. The divergent beam at the Cassegrain focus is collimated by an off-axis paraboloid (OAP-1) and sent to a fast steering mirror (FSM), which rapidly corrects the tip-tilt component of image motion. The beam is then sent to the deformable mirror (DM), which corrects higher-order components of image deformation. A second off-axis paraboloid (OAP-2) focuses the corrected beam into a science camera, typically working in the near infrared; a dichroic picks off the visible wavelengths and sends them into a wavefront-sensor camera that uses the point reference star to derive correction commands used by the fast steering mirror and the deformable mirror. The AO system provides an image at the science camera in which atmospheric phase fluctuations and aberrations in the telescope optics are substantially corrected.

2. ADAPTIVE OPTICS

The concept of adaptive optics was proposed by Babcock[1] in 1953. He envisioned a deformable mirror placed optically conjugate to the telescope pupil, so that rapid changes in the figure of the deformable mirror could be made to compensate for phase errors occurring over the pupil. These phase errors would be detected by observations of a point reference star with a wavefront sensor capable of sensing variations from the desired plane wavefront. Babcock's proposal was remarkably prescient and similar to the modern approach, but little was done in this area for years due to a lack of available technology to implement these ideas. Some early progress with practical systems was made in the 1970's, largely as a result of military interest in the problem, and the technological spinoffs that resulted started to be incorporated into useful astronomical systems in the late 1980's[2,3].

In Figure 1 we show a schematic of an adaptive optics system for astronomical use. The system as drawn is mounted at the telescope's Cassegrain focus, as will be the case with the system being built at the Jet Propulsion Lab for the Palomar 200" telescope[4]. Other possibilities include mounting at a fixed Nasmyth focus, as at the Keck 10 meter telescope[5], where the adaptive optic instrumentation must then move as the telescope tracks in azimuth but need not tip with telescope altitude; this may afford better immunity to flexure, to which AO systems are quite sensitive. Light from the telescope is directed onto a fast-steering (tip-tilt) mirror, then onto the multi-actuator deformable mirror, then the resultant corrected infrared beam is directed onto the science camera. Typical DM's now being incorporated in astronomical systems have several hundred actuators (349 for the systems being built for both Palomar and Keck), permitting quite high-order correction. A dichroic or beam-splitter in the final beam directs some light from the reference point star onto the wavefront sensor camera, which derives the commands to drive the tip-tilt (FSM) mirror and deformable mirror, with the help of an algorithm called the reconstructor. The beam into the science camera is now substantially corrected for telescope aberrations and atmospheric seeing when the AO control loops are locked. Typically, for adaptive systems operational now and planned for the near future, wavefront sensing is done at optical wavelengths, while science cameras are operated in the near-infrared, where seeing perturbations are smaller and slower; the non-dispersive nature of the atmosphere makes this possible.

The reconstructor is an algorithm for converting the wavefront information measured by the wavefront sensor into commands controlling the motion of actuators on the deformable mirror. It may be quite involved depending on the type of wavefront sensor and deformable mirror used, and must operate in real time at high speed (typically millisecond timescales). The connection between the tip-tilt sensor and the fast steering mirror is much simpler, although also operated in a high-speed loop, as the tip-tilt sensor consists in some systems merely of a quad-cell arrangement of avalanche photodiodes that indicate when corrections to the centering of the guide star are required. The reason for separating these two functions is practical rather than conceptual. Tip-tilt is just one component of wavefront aberration, but generally contains by far the bulk of the power, and so would overwhelm the travel of the actuators of the deformable mirror; it is nonetheless easily handled by a fast steering mirror.

3. VIDEO IMAGING OF TURBULENCE AT THE PALOMAR 200" TELESCOPE

Astronomical experience indicates that atmospheric seeing is highly variable with geographic location, time of year, and time of night at a given site, and is by no means necessarily ideal (i.e. corresponding to a Kolmogorov spectrum of turbulence) in practice. Clearly, direct experimental determination of the specific character of seeing at our site would be useful in assessing the conditions that the planned adaptive optics system will have to handle.

To this end, we carried out extensive video imaging of single stars and clusters with the Palomar 200" reflector. A standard video camera with a frame rate of 30 Hz recorded data onto Hi-8 videotape. Our equipment was mounted at the f/15.8 Cassegrain focus, where the plate scale is 2.6"/mm; on a focused image, the total field of view was roughly 63"×47" in a 640×480 pixel format. Our video of in-focus stellar clusters may be analyzed to measure rapid shifts in stellar positions over the imaged field. These shifts, and their correlations as a function of stellar separation, are fundamental diagnostics of seeing. Two alternative techniques were used to quantitatively study the stellar-cluster video: the autoguider hardware discussed in §4, and the frame-grabbing/IRAF-reduction approach discussed in §5. We also obtained Schlieren images of single stars (for gradient wavefront sensing...see §6) and out-of-focus images of single stars (for curvature wavefront sensing...see §7). For the former observations, a knife-edge was placed in the focal plane and the light was reimaged to yield an image of the telescope pupil.

4. AUTOGUIDER HARDWARE ANALYSIS OF STELLAR CLUSTERS

The Palomar 200" telescope uses an "autoguider" circuit to automatically maintain telescope pointing on a bright reference star not far from the field of scientific interest. This circuit operates on a standard video signal and establishes a square search box within which it sums intensity from pixels along the video sweep on one side of the box, and then subtracts intensity from those on the other. The resulting total signal formed for each of the 16 horizontal lines of the 16x16 search box is an un-normalized, flux-weighted determination of which side of the search-box center line the guide star is located. A similar summation is performed in the vertical direction to complete the quadrant detection. Within a certain range of relative scales (stellar seeing diameter to search window), the quadrant detection may be taken as a useful measure of stellar position relative to the center of the search box.

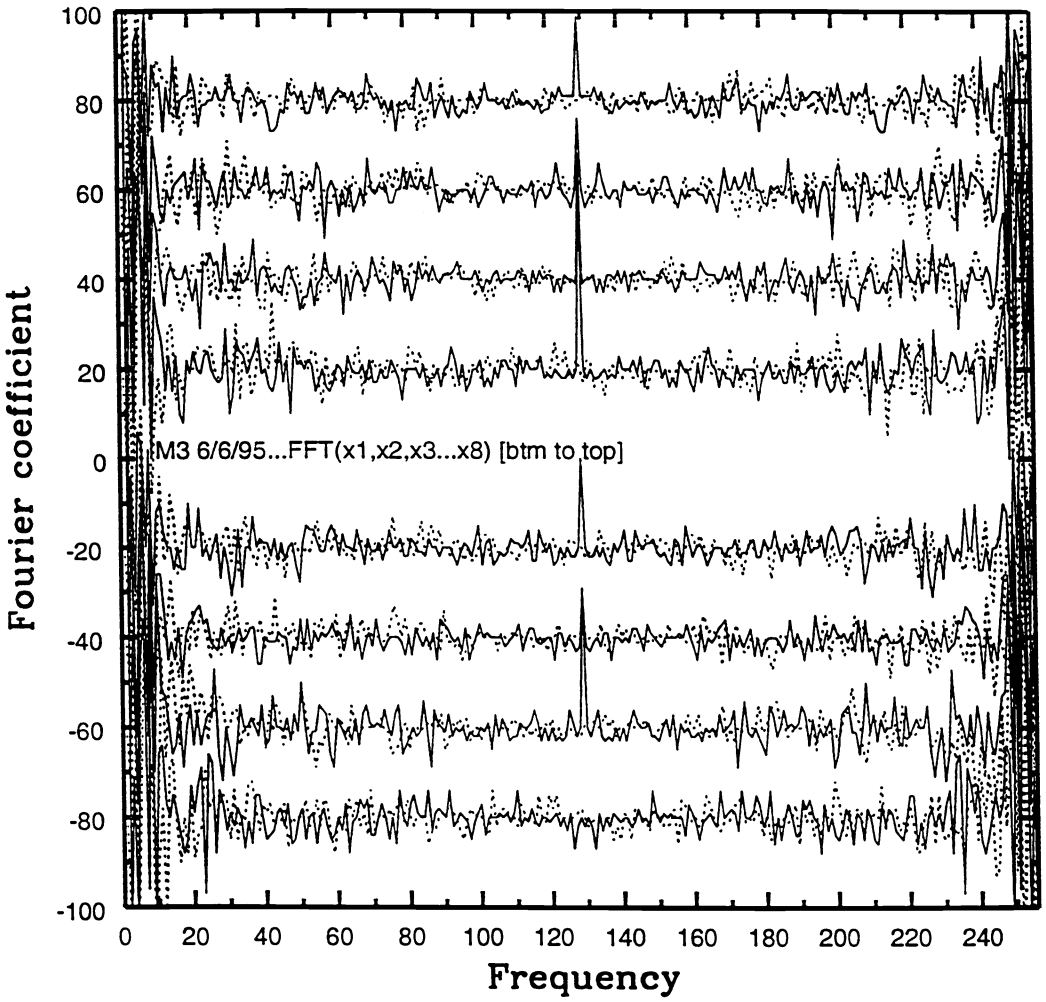

FIG. 2 – Discrete Fourier transform of all 8 channels from the autoguider box x-position time series (solid lines are real components; dashed lines are imaginary) spanning 256 samples (8.5 seconds of time). The DC point is at frequency=1; the highest physical frequencies lie in the center of the plot. The spike at frequency=129 corresponds to image jitter at the frame rate, 30 Hz.

The usefulness of this hardware for studying stellar motions under the effect of atmospheric seeing is immediately apparent. Moreover, the algorithm is sufficiently simple that positions may be evaluated and stored at the video playback rate. An 8-channel (8-search-box) parallel version of this circuit was developed that yielded positions in each video frame for 8 stars chosen arbitrarily in the field. Results with this system for the stellar cluster M3 show well-behaved position measurements (e.g. distributions of y-position versus x-position are round); the long-term scale

of the seeing position wander has an amplitude of about 1". Care must be taken when interpreting this number, however, due to the non-linearities in the behavior of a quadrant-detection mechanism[6]: in general, positions returned are affected by the scales of the instantaneous seeing blur spot and of the search box.

We performed a discrete Fourier transformation of the stellar positions returned by the 8-channel autoguider box, as a means of searching for irregular behavior and signatures of strong common-mode motions, such as telescope windshake. The transform for the x-position values from all 8 channels is shown in Figure 2. For the conventions of the transform used here, the DC point is found at the frequency index of 1, while the highest physical frequency lies at the center of the frequency axis range. A spike of power is seen at the video frame rate; this is expected from the interleaving of frames, and is purely an artifact of the video recording process. A mechanical resonance in the telescope is known to exist at about 3 Hz, which would correspond to a frequency index of 13 on this plot; there may be a discrete component of power there, but it is difficult to distinguish from the general rising 1/f noise spectrum at low frequencies.

Interpretation of stellar-cluster video data reduced with the adapted autoguider hardware is somewhat complicated by the nonlinear conversion from intensity-weighted quadrant detection to centroid position. For this reason, we will concentrate here on deductions from a more straightforward centroiding scheme presented in the next section. Interestingly, a relatively simple modification can be made to the autoguider hardware to yield true centroids while sacrificing little speed. A multiplication chip can be incorporated in the circuit performing the running summation of intensity so that it integrates the instantaneous product of signal intensity and position offset within the search box. We have modified one channel of our 8-channel device for this approach, and initial tests are encouraging.

5. FRAME-GRABBING/IRAF ANALYSIS OF STELLAR CLUSTERS

A straightforward approach to analyzing video of stellar clusters whose positions are corrupted by atmospheric turbulence is to parse each frame in software for positions of all sufficiently bright stars. In this approach, full individual frames are digitized by frame-grabbing hardware and imported into a data analysis package for fitting of true stellar centroids. As compared to the modified autoguider circuitry, position fitting by this route is somewhat laborious, because real-time frame-grabbing is difficult to achieve; however, a true centroid is determined, and additional analysis may be carried out with a great deal of flexibility. For position fitting, we have used the IRAF package [distributed by NOAO, which is operated by AURA Inc. under contract to the National Science Foundation], which has simple routines for calculating stellar centroids within specified search boxes. IRAF is able to output the results of position fits in a convenient format for further processing by custom software of our own design.

A typical field for the stellar cluster M3 is shown in Figure 3. This image is one of 29 consecutive frames, spanning roughly one second of time, selected from a very large set of data obtained at about 9 PM on 6 June 1995, in conditions of rather good seeing (perhaps one arc second). In our analysis of these frames, we have fitted for the positions of the seven brightest stars. After stellar position centroids are obtained for all frames of the time series, custom software is used to calculate the statistics of the stellar motions. The seeing-induced motions of single stars imaged at wavelength λ with a telescope of diameter D may be used to deduce Fried's parameter r_0, a basic measure of seeing quality, from the relation $\Delta\theta_{rms} = 0.43(\lambda/D)(D/r_0)^{5/6}$, where $\Delta\theta_{rms}$ is the one-axis rms angular image motion[7]. For the time series considered here, $r_0 = 12$ cm is derived, which is a reasonable value for relatively good conditions. With respect to image motions due to windshake, frame-grabbing errors, or position-fitting errors, this value is a lower limit; all of these errors will worsen apparent atmospheric image motions. However, the restriction to 30 Hz bandwidth imposed by use of the standard video recording rate will mask high-frequency image motions that would correspond to a smaller (worse) value of r_0. A more careful treatment would also apply an FFT filter to remove the jitter at the video frame rate that is visible as the spike in Figure 2.

By comparing the variations in relative positions of stars at different positions in the field, the amount of tilt anisoplanatism may be derived. This quantity expresses the decorrelation of the tip-tilt components of seeing with separation of two lines of sight; this is extremely relevant to adaptive optics, where the lines of sight in question involve the science object and the fiducial guide star. A convenient figure of merit is the isokinetic angle θ_k, defined analogously to the isoplanatic angle except that rms phases due to tip/tilt alone become equal to 1 radian rms at this object separation. Owing to this relaxed definition, the isokinetic angle is larger than the isoplanatic angle; in

a laser-guide-star adaptive optics system, the natural guide star used to provide tip/tilt information need only lie within the isokinetic angle of the science object.

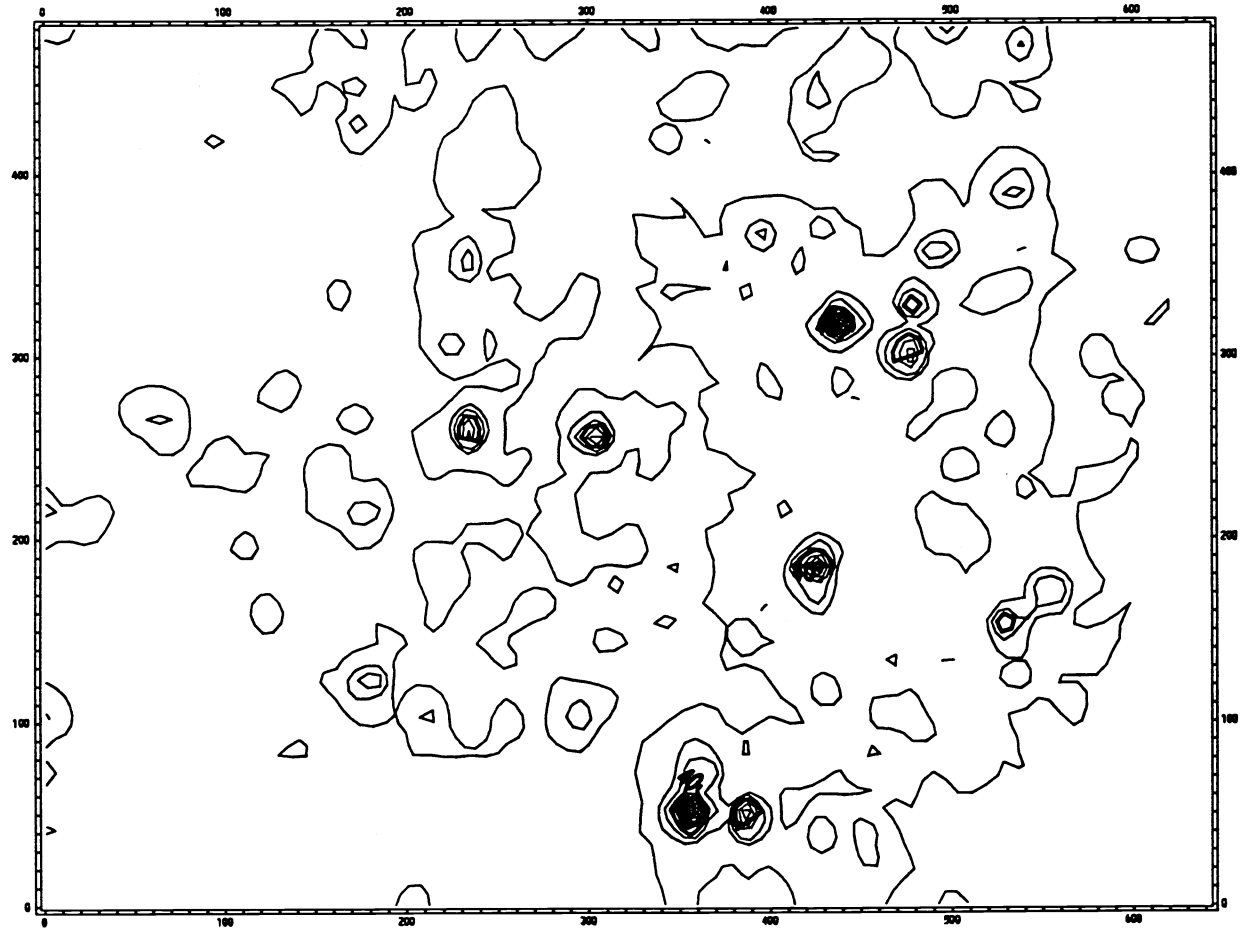

FIG. 3 – Single frame from video of the stellar cluster M3. The field of view spans roughly 63"×47"; at least 7 stars are bright enough to yield centroid (position) measurements.

To evaluate tilt anisoplanatism, the following procedure is used. Within each frame of a time series, the radial separation of each pair of stars bright enough to permit position analysis is evaluated and stored; the mean and standard deviation of the radial separation for each pair are then evaluated by averaging over all frames. A plot of that standard deviation against mean radial separation should rise at larger stellar separations, as motions induced by atmospheric fluctuations become less correlated. For the 29-frame time series (corresponding to one second of time) such a plot is shown in Figure 4.

The differential stellar motions may be converted to relative phase shifts as a function of angular separation, and these yield an estimate of the isoplanatic angle, θ_0, via $\sigma_\phi = (\Delta\theta/\theta_0)^{5/6}$, where stars separated by $\Delta\theta$ exhibit rms relative phase variations of σ_ϕ. For the 29-frame data set on M3, we find $\theta_0 = 2.5$". Comparing r_0 and θ_0, which in a single-turbulent-layer model are related by[8] $\theta_0 = 0.314 r_0/h_0$ for a turbulent layer at distance h_0 (roughly equal to layer height for observations near the zenith), we derive a scale height of the dominant turbulent component of roughly 3 km.

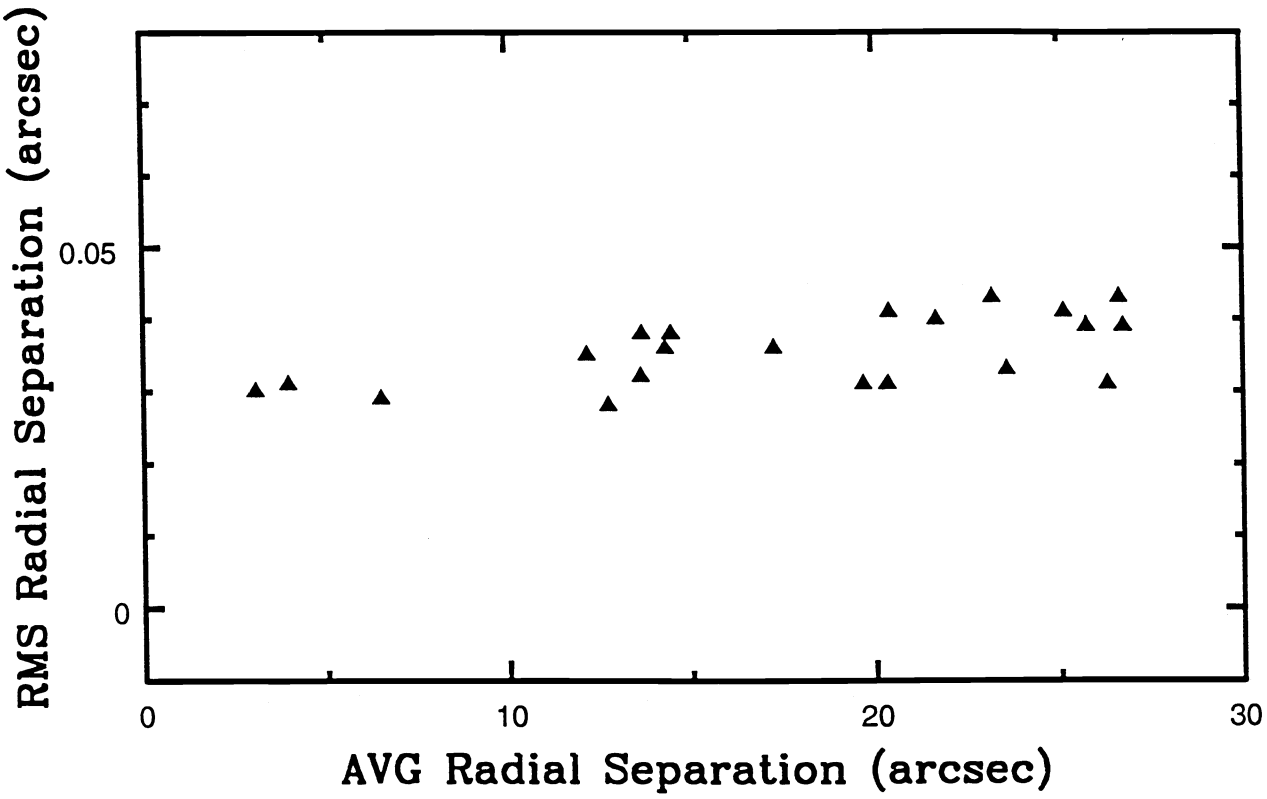

FIG. 4 – RMS spread in radial separation plotted against average radial separation for each pairwise combination of 7 stars in our field in the M3 stellar cluster. The rise at larger stellar separations is indicative of the decorrelation of stellar motions at larger separation angles.

6. GRADIENT WAVEFRONT SENSING

The most common choice of wavefront sensor in the many adaptive optics systems now under design or construction is the Shack-Hartmann approach. This approach is to be implemented in the system being built at JPL for the Palomar 200" telescope and the system being built for the Keck II telescope on Mauna Kea. In a Shack-Hartmann wavefront sensor, the telescope pupil is reimaged onto an array of lenslets, with typically 16 lenslets across the diameter of the pupil, and these focus light from subapertures of the pupil onto the wavefront sensing camera. The spot from each lenslet/subaperture is ideally placed on the intersection of four pixels in the wavefront sensing camera, so a quad-cell position detector for the focused light from that lenslet is obtained. The deviations of each spot are then a measure of local tip-tilt over the subaperture, or, equivalently, of the phase gradient (or first derivative of phase) in two dimensions. With an appropriate reconstructor algorithm, these local phase gradients can be connected into a phase map across the pupil that in turn may be used to drive the deformable mirror.

Another method for sensing the phase gradient within the telescope pupil with rather high spatial resolution is the knife-edge (or Foucault or Schlieren) technique. Here a sharp edge is placed across the focal-plane image of a single unresolved star, and an image of the telescope pupil is formed with additional reimaging optics. The spatial resolution is now limited by the number of pixels in the wavefront-sensing camera, not by the number of lenslets; however, this approach is not favored for practical adaptive optics systems because the phase gradient is sensed only in a single direction, perpendicular to the knife-edge. This limitation may be overcome with a rather complicated optical scheme and a second knife-edge, but the resulting division of the wavefront causes a loss of sensitivity compared to the Shack-Hartmann approach.

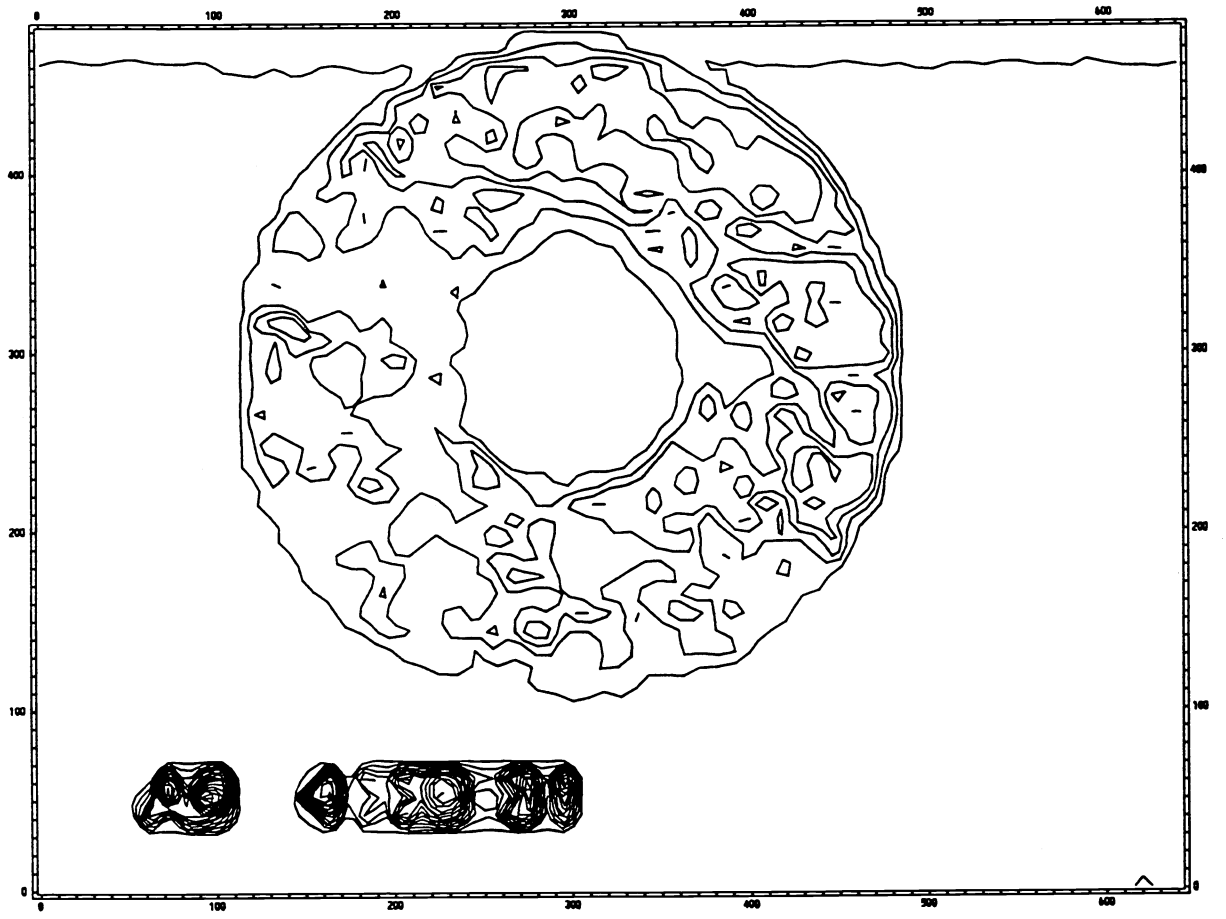

FIG. 5 – Single frame from video of phase gradient imaged over the pupil of the 200" Palomar telescope. A single unresolved star is observed with a knife-edge in the focal plane; the pupil is then re-imaged with additional optics. The outer edge of this annular pupil is formed by the diameter of the primary mirror; the inner edge is formed by the diameter of the secondary (the coherent structures at lower left are labels produced by time-stamping the videotape).

Despite this sensitivity disadvantage, a one-dimensional knife-edge system is relatively easy to implement, and so was incorporated for some of our atmospheric turbulence imaging at Palomar. A typical data frame representing a 1/30 second integration is shown in Figure 5. The video was frame-grabbed from our Hi-8 videotape, then imported into the astronomical processing package IRAF for this display. A correlation analysis was carried out by exporting the data frames from IRAF and auto- or cross-correlating them with custom external software. Inspection of the knife-edge video gives an impression that frozen structures are blowing across the aperture with a unique direction and speed that presumably corresponds to the dominant turbulent layer in the atmosphere. The two-dimensional cross-correlation of frames separated by short time intervals yields an offset magnitude and direction to the correlation peak from which a flow can be calculated, and this flow agrees with the subjective impression found on inspection.

7. CURVATURE WAVEFRONT SENSING

An alternative means of extracting the phase across a telescope pupil was first elucidated by Beckers and Williams[9] (see the review article by Beckers[10] for an updated derivation), and uses a particularly simple hardware setup. If the image of a point reference star is observed well away from the focal point, far enough that a geometrical optical

treatment of the rays is sufficient, it may be shown by a fairly simple construction that bright and dark patches in the image correspond to regions of unusual curvature of the reflecting surface, or, equivalently, of the incident wavefront. So these simple out-of-focus images provide measurements of the second derivative of the phase across the pupil, in contrast to the knife-edge measurement of the first derivative; furthermore, no loss of sensitivity is suffered from light blockage in the spatial filter plane. Considerable astronomical success has been realized with relatively simple systems employing curvature wavefront sensors[11]. They have generally also employed "bimorph" deformable mirrors, which differ in response from the more conventional PMN-actuator mirrors in that the application of a drive voltage to a bimorph directly results in a change of curvature. The natural match between curvature wavefront sensing and bimorph mirrors leads to an unusually simple reconstructor algorithm.

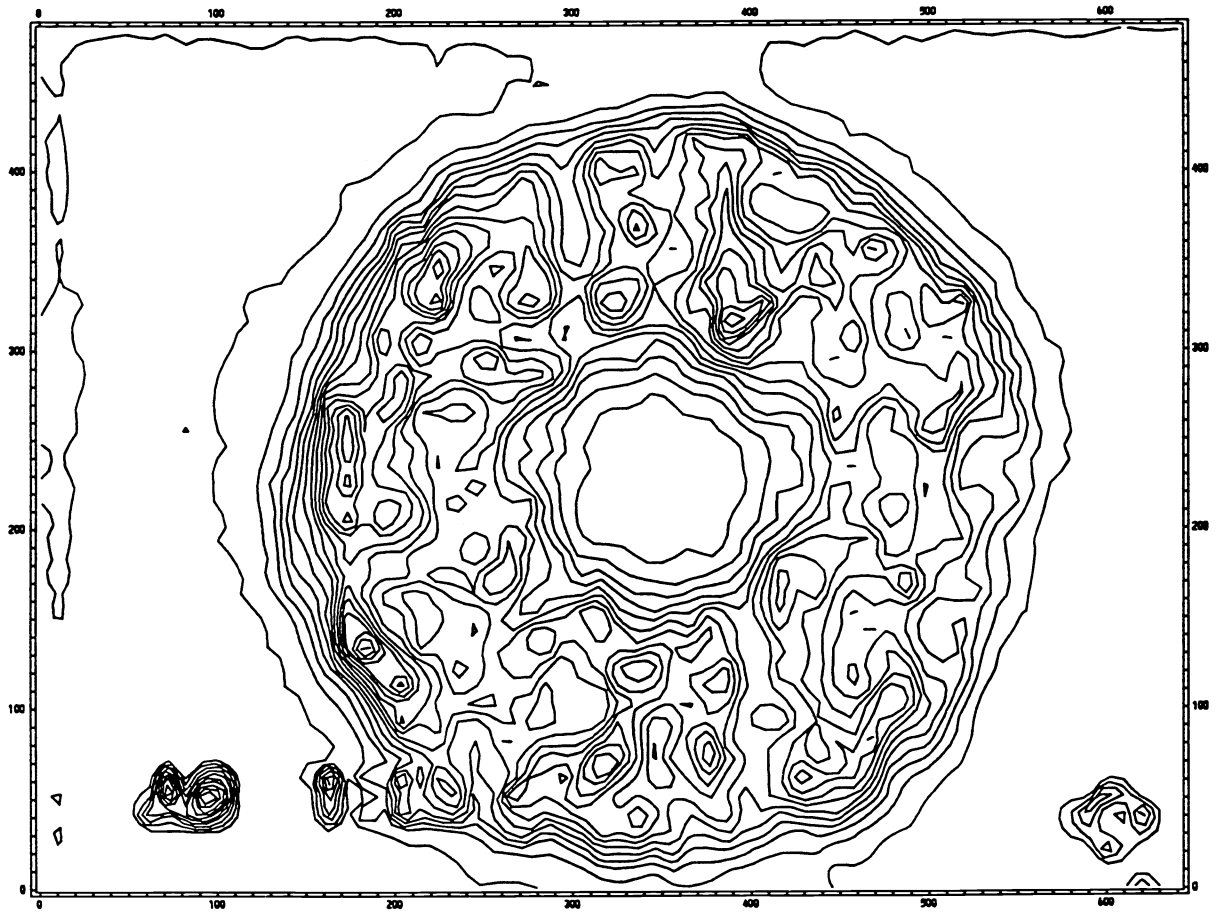

FIG. 6 – Single frame from video of phase curvature (second derivative) imaged over the pupil of the 200" Palomar telescope. A single unresolved star is observed with the telescope well out of focus (the coherent structures near the bottom of the frame are labels produced by time-stamping the videotape).

A typical frame of a single unresolved star obtained at large defocus at the Palomar 200" telescope is shown in Figure 6. In some data analyzed, the scale is such that the entire pupil cannot be covered at once, but this greater resolution across the pupil actually makes the search for coherent feature motion somewhat easier. As with knife-edge (phase-gradient) video, the phase distortions appear to be complex but dominated by a single component possessing a certain flow direction and speed that varies from one night of observation to another. The characteristic velocity estimated for this dominant frozen-in flow matches the result of a quantitative cross-correlation analysis. Solving for a phase map from our curvature video might be useful for predicting adaptive optics system performance; this would be similar in implementation to a curvature wavefront sensor under development for calibration purposes for the Palomar 200" adaptive optics system. Future efforts will also be directed towards extracting additional underlying

turbulence components in both knife-edge and phase-curvature images that can be seen in visual inspection of the video.

8. LARGE REFOCUS EVENTS

Even a fairly cursory visual inspection of the turbulence video obtained at Palomar reveals some remarkable behavior. One example may be observed and quantified with out-of-focus video of stellar clusters such as M3. One occasionally sees a synchronized growth of all the stellar annuli and a subsequent return to their original size, taking place over a period of a second or two...essentially a substantial focusing or defocusing of the image that is uniform across the entire field. These events may be interpreted as passage of coherent parcels of air roughly matched in size to the 200" telescope aperture, with temperature (and thus refractive index) substantially different than the average for the layer in which they are found. Quantitatively, we see the out-of-focus annulus of each star in our cluster field change diameter by an amount δx, corresponding to a longitudinal focal shift of $\delta f = f/\# \, \delta x$; expressed in terms of wavefront phase delay $\delta\xi$ at the extreme edge of the circular phase front that gives focal shift, this is $\delta\xi = (8f/\#)^{-1} D(\delta f/f)$. For some of these extreme events (seen under conditions of Santa Ana winds, which are generally associated with quite poor seeing conditions at Palomar), $\delta x \sim 0.39$ mm, so for the $f/16$ Cassegrain focus of the 200" telescope the defocus amplitude is roughly 3 μm wavefront error at the edge of the pupil. This is a large fraction of the total correction capability (throw) of an individual actuator on the deformable mirror to be used in the Palomar adaptive optics system ($\sim$ 8 μm of wavefront) and might be problematic if a significant portion of the throw were already engaged in correction of quasistatic telescope aberrations; however, events this extreme are rare and may not occur under all weather conditions.

9. ACKNOWLEDGMENTS

Wayne Waller of Caltech's Campus Computing Organization assisted with frame-grabbing our video data, and Richard Lucinio developed the 8-channel autoguider electronics. Rich Dekany provided helpful insights into various aspects of adaptive optics, and Anand Sivaramakrishnan advised on IRAF analysis of seeing data.

10. REFERENCES

1. H. W. Babcock, "The Possibility of Compensating Astronomical Seeing", *Pub. Astron. Soc. Pac.*, vol. 65, pp. 229-236, 1953.

2. J. M. Beckers, F. J. Roddier, P. R. Eisenhardt, L. E. Goad, K.-L. Shu, *Proc. Soc. Photo-Opt. Inst. Eng.*, vol. 628, p. 290, 1986.

3. G. Rousset, J. C. Fontanella, P. Kern, P. Gigan, F. Rigaut, P. Lena, C. Boyer, P. Jagourel, J. P. Gaffard, F. Merkle, "First Diffraction-Limited Astronomical Images with Adaptive Optics", *Astron. Astrophys.*, vol. 230, pp. L29-L32, 1990.

4. R. G. Dekany, "The Palomar Adaptive Optics System", in *Adaptive Optics*, Vol. 13, 1996 OSA Technical Digest Series (Optical Society of America, Washington, DC, 1996), pp. 40-42.

5. P. Wizinowich, D. S. Acton, A. Gleckler, T. Gregory, P. Stomski, K. Avicola, J. Brase, H. Friedman, D. Gavel, C. Max, "W. M. Keck Observatory Adaptive Optics Facility", in *Adaptive Optics*, Vol. 13, 1996 OSA Technical Digest Series (Optical Society of America, Washington, DC, 1996), pp. 8-10.

6. R. K. Tyson, "Principles of Adaptive Optics" *(New York: Academic Press)*, 1991.

7. D. G. Sandler, S. Stahl, J. R. P. Angel, M. Lloyd-Hart, D. McCarthy, "Adaptive Optics for Diffraction-limited Infrared Imaging with 8-m Telescopes", *J. Opt. Soc. Am. A*, vol. 11, pp. 925-945, 1994.

8. D. L. Fried, "Anisoplanatism in Adaptive Optics", *J. Opt. Soc. Am.*, vol. 72, pp. 52-61, 1982.

9. J. M. Beckers, J. T. Williams, "Intensity Rings in Out-of-Focus MMT Star Images", *MMT Technical Memorandum*, 79-1, 1979.

10. J. M. Beckers, "Adaptive Optics for Astronomy", *Ann. Rev. Astron. Astrophys.*, vol. 31, pp. 13-62, 1993.

11. F. Roddier, M. Northcott, J. E. Graves, "A Simple Low-Order Adaptive Optics System for Near-Infrared Applications", *Pub. Astron. Soc. Pac.*, vol. 103, pp. 131-149, 1991.